

Stability of Atomic Condensed Systems with Attractive Two-Body Interactions

L. Tomio¹, V. S. Filho¹, A. Gammal², and T. Frederico³

¹ Instituto de Física Teórica, Universidade Estadual Paulista, 01405-900, São Paulo, Brazil

e-mail: tomio@ift.unesp.br, vsf@ift.unesp.br

² Instituto de Física, Universidade de São Paulo, 05315-970, São Paulo, Brazil

e-mail: gammal@if.usp.br

³ Instituto Tecnológico da Aeronáutica-, CTA, 12228-900, São José dos Campos, Brazil

e-mail: tobias@fis.ita.br

Received September 14, 2002

Abstract—In the present report, we review recent investigations that we have conducted on the stability of atomic condensed systems, when the two-body interaction is attractive. In particular, the dynamics that occurs in the condensate due to nonconservative terms is considered in the context of an extension of the mean-field Gross–Pitaevskii approximation. Considering the relative intensity of the nonconservative parameters, chaotic and solitonic solutions are verified. Also discussed is the possibility of a liquid–gas phase transition in the presence of positive three-body elastic collisions.

1. INTRODUCTION

Bose–Einstein phase-transition of ultracold trapped atoms to stable condensed states has been verified experimentally in several cases [1–3]. However, a condensed state of atoms with a negative s -wave atom–atom scattering length would be unstable for a large number of atoms [4]. So, it was indeed observed in ⁷Li gas [3], for which the s -wave scattering length is $a = (-14.5 \pm 0.4)$ Å, that the number of allowed atoms in the condensed state was limited to a maximum value between 650 and 1300, which is consistent with the mean-field prediction [4]. We should also note that, actually, by means of Feshbach resonance techniques (see Courteille *et al.* [5] and references therein), one has the ability to control the scattering length, varying it from positive to negative values, as was shown recently in the Bose–Einstein condensation of ⁸⁵Rb [6]. Condensed systems with attractive interaction ($a < 0$) have been investigated by our research group in the context of the Gross–Pitaevskii (GP) formalism and extensions. More recently, we have also considered the case of repulsive two-body interactions. In the present report, we summarize some of our main results, particularly those concerned with the stability of condensates. In our approach, we consider two kinds of generalizations of the GP formalism, by considering the addition of a real quintic term in the nonlinear effective interaction [7] and also by considering nonconservative (linear, cubic, and quintic) terms [8, 9]. Since the corresponding nonlinear Schrödinger equation (NLSE), with trap, is nonintegrable, we had to use advanced stable numerical methods to solve it for the static [7, 10–13] and dynamical cases [8, 9, 14]. Variational approaches have also been considered in our analysis [7, 13, 14].

In the following, we first present the general formalism that we have considered, with some discussion on specific cases; next, in Section 3, we present results obtained for the stationary case of the GP formalism with the addition of a real quintic term in the effective interaction. Two subsections have been included: in the first, we consider general nonspherical traps; in the second, we consider the influence of anharmonic terms in the original harmonic trap. In Section 4, we present results obtained for the dynamical case, considering three-dimensional symmetric traps, followed by our concluding remarks.

2. EXTENDED GROSS–PITAEVSKII MEAN-FIELD APPROXIMATION

The usual mean-field approximation that is considered to describe condensates of dilute bosonic gases is given by the GP formalism. We considered an extension of the usual GP approximation, which is an NLSE with cubic and quintic nonlinear terms, as well as non-conservative parts:

$$\begin{aligned} i\hbar \frac{\partial \Psi(\mathbf{r}, t)}{\partial t} = & \left[-\frac{\hbar^2}{2m} \nabla^2 + V(\mathbf{r}) \right. \\ & \left. + \frac{4\pi\hbar^2 a}{m} |\Psi(\mathbf{r}, t)|^2 + \lambda_3 |\Psi(\mathbf{r}, t)|^4 \right] \Psi(\mathbf{r}, t) \\ & + i[G_\gamma - G_\mu |\Psi(\mathbf{r}, t)|^2 - G_\xi |\Psi(\mathbf{r}, t)|^4] \Psi(\mathbf{r}, t). \end{aligned} \quad (1)$$

The wave function $\Psi(\mathbf{r}, t)$ is normalized to the number of particles N , which is a constant when the nonconservative terms are zero. In Eq. (1), a is the two-body scattering length, m is the atomic mass, and λ_3 is

the strength of the effective three-body interaction. The following nonconservative terms were considered: a linear feeding G_γ and two dissipative terms given by G_μ , related to dipolar relaxation, and G_ξ , a three-body recombination factor. These parameters are assumed to be constant and positive, for which the corresponding signs are given in Eq. (1). For the trapping potential $V(\mathbf{r})$, we consider the usual harmonic shape, which in general can be nonsymmetric and given by $V(\mathbf{r}) = \frac{m}{2}[\omega_x^2 x^2 + \omega_y^2 y^2 + \omega_z^2 z^2]$. In the present communication, we report only studies for systems with attractive two-body interaction ($a < 0$).

3. STATIONARY CONDENSATES WITH NEGATIVE SCATTERING LENGTH

In this section, we consider the case where the nonconservative terms of Eq. (1) are zero ($G_\gamma = G_\mu = G_\xi = 0$): N is constant and we can substitute the time-dependent wave function by $\Psi(\mathbf{r}, t) = e^{-i\mu t/\hbar}\psi(\mathbf{r})$, where μ is the chemical potential (single particle energy). In the following, we first consider a symmetric case with a repulsive three-body term; next, we consider the more realistic nonsymmetric case, with $\lambda_3 = 0$.

3.1. Symmetric Case, with $\lambda_3 > 0$

By considering a symmetric harmonic trap (with $\omega = \omega_x = \omega_y = \omega_z$), with a nonzero repulsive three-body term ($\lambda_3 > 0$), for the conservative case, Eq. (1) is reduced to

$$\mu\psi(\mathbf{r}) = \left[-\frac{\hbar^2}{2m}\nabla^2 + \frac{m}{2}\omega^2 r^2 - \frac{4\pi\hbar^2|a|}{m}|\psi(\mathbf{r})|^2 + \lambda_3|\psi(\mathbf{r})|^4 \right]\psi(\mathbf{r}). \quad (2)$$

The total energy of the system is given by

$$E = \int d^3r \left\{ \frac{\hbar^2}{2m}|\nabla\psi(\mathbf{r})|^2 + \frac{m}{2}\omega^2 r^2|\psi(\mathbf{r})|^2 - \frac{2\pi\hbar^2|a|}{m}|\psi(\mathbf{r})|^4 + \frac{\lambda_3}{3}|\psi(\mathbf{r})|^6 \right\}. \quad (3)$$

The central density of the system can be obtained directly from the solution to the above equation: $\rho_c = |\psi(0)|^2$. The chemical potential and the three-body strength, respectively, are redefined by

$$\beta \equiv \frac{\mu}{\hbar\omega} \quad \text{and} \quad g_3 \equiv \lambda_3\hbar\omega \left[\frac{m}{4\pi\hbar^2 a} \right]^2. \quad (4)$$

Figure 1 shows, in a compact form, the main results obtained for the total energy E , mean square radius $\langle r^2 \rangle$, central density ρ_c , and chemical potential μ . They are

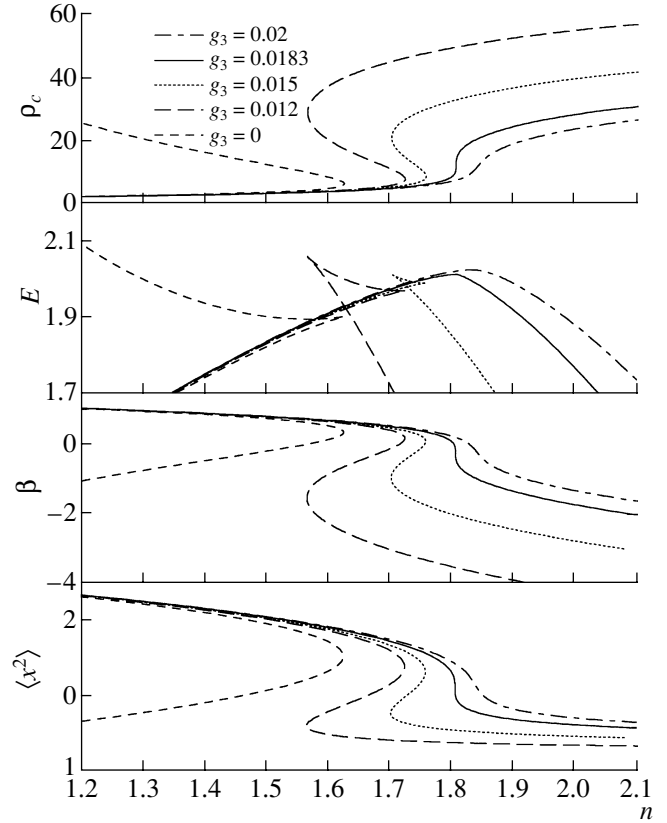


Fig. 1. Observables of the condensate versus $n \equiv 2N|a|\sqrt{2m\omega/\hbar}$, related to the number N of particles. The given values should be multiplied by the respective units: $(m\omega/\hbar)/(4\pi|a|)$ for the central density ρ_c ; $(N\hbar\omega/n)$ for the total energy E ; $\hbar\omega$ for the chemical potential β ; and $\hbar/(2m\omega)$ for the mean square radius $\langle r^2 \rangle$. The values of g_3 are given in the upper frame.

given as a function of the parameter n , which is related to the number of particles: $n \equiv 2N|a|\sqrt{2m\omega/\hbar}$. The results are given for several values of the three-body interaction parameter g_3 . These results were obtained by a full numerical calculation based on the shooting Runge–Kutta method [7]. They show the existence of two distinct phases in the condensate, when $\lambda_3 > 0$. As one can observe in the framework corresponding to the density variation, the system becomes more than three times denser than the original one when a transition is made. Also, for $0 < g_3 < 0.0183$, we observe that the density ρ_c shows back bending typical of a first-order phase transition. The curves obtained show a clear dependence of the phase transition with the g_3 strength, and, mainly in the density graph, it is possible to verify that there is a region of low density (gas) and a region of high density (liquid). The two-phase regime disappears for $g_3 > 0.0183$, as one can see in Fig. 1. Qualitatively, the behavior of the system was reproduced considering a variational approach (see [7]).

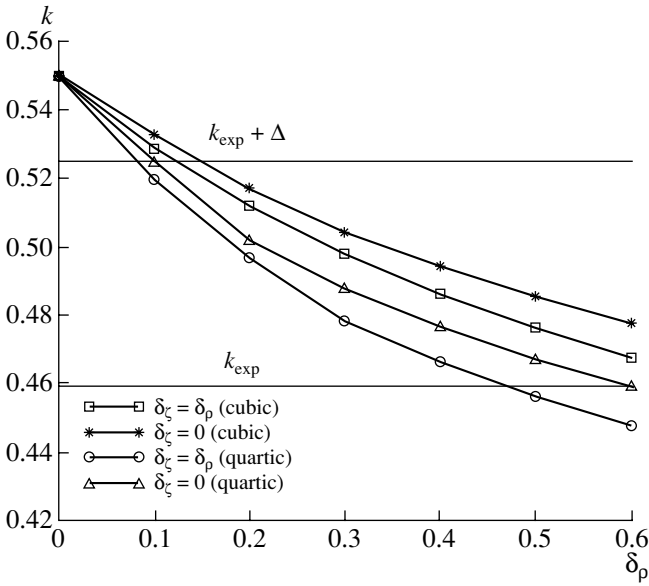


Fig. 2. Variation of k (related to the critical number of atoms N_c) as a function of the deviation in the perpendicular direction, given by δ_p . The corresponding deviations in the z direction, δ_z , are given inside the figure. The position of the experimental k and the corresponding positive error bar (Δ) are also indicated.

3.2. Nonsymmetric Case, with $\lambda_3 = 0$

In this subsection, we consider the more realistic case of nonsymmetric traps that have been employed in experiments of atomic condensation with negative two-body scattering length. In Eq. (1), the nonconservative terms are zero, and we also have not considered elastic three-body interaction, such that $\lambda_3 = 0$. Our investigation, in this case, is concentrated in verifying the influence of the trapping symmetry on the critical number of atoms. Motivated by the observed discrepancy between theoretical predictions and experimental results, in the maximum critical number of atoms, as reported in [6], we considered in [10] the cylindrical symmetry employed in [6], where $\omega_\perp \equiv \omega_x = \omega_y \neq \omega_z$ and $\omega^3 \equiv \omega_\perp^2 \omega_z$. By considering this cylindrical symmetry, we show that the maximum critical number of atoms in the condensate, N_c , parametrized by $k \equiv N_c |a| \sqrt{(m\omega/\hbar)}$, is $k = 0.55$. This represents a reduction of about 4.4% from the number obtained with a spherical symmetric trap ($k = 0.574$). Next, we also considered the influence of anharmonic terms added to the trapping potential. The effect of a deviation of the trap potential from the harmonic behavior is analyzed by considering the following expression for a cylindrical trap ($r_\perp \equiv \sqrt{x^2 + y^2}$):

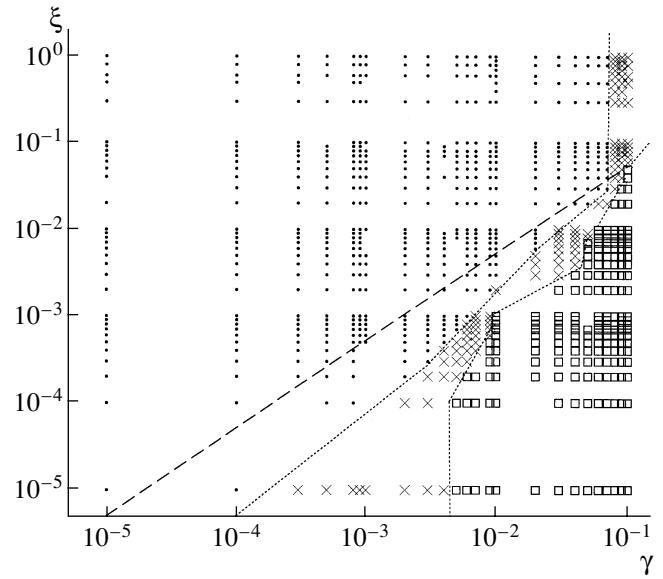


Fig. 3. Diagram for stability, according to the criterion of [15], considering the nonconservative parameters for the feeding, γ , and dissipation, ξ . Unstable results are represented by \times and boxes, where the boxes identify chaotic solutions. The dots are for stable results. The two dotted guidelines split the regions. The dashed line splits the graph into two regions according to a variational approach (see [8, 9]); in the upper part, the results are stable; in the lower part, unstable.

$$V^{(v)}(r_\perp, z) = \frac{m}{2} [\omega_\perp^2 r_\perp^2 (1 + \delta_p (r_\perp/l_0)^v) + \omega_z^2 z^2 (1 + \delta_z (z/l_0)^v)], \tag{5}$$

where $l_0 \equiv \sqrt{\hbar/(m\omega)}$. The magnitudes of the distortions added to the harmonic potential in the directions r_\perp and z are given by δ_p and δ_z for both cubic ($v = 1$) and quartic ($v = 2$) distortions.

Figure 2 shows the behavior of k as the magnitude of the anharmonic term increases. For both cases that we have cubic or quartic distortions, we have considered the case $\delta_z = \delta_p$ and $\delta_z = 0$. As one can observe, the higher the anharmonic parameter, the smaller the critical number of condensed atoms. Considering the JILA experiment [6], we should also note that, in order to obtain the theoretical results for k within the region covered by the experimental error bars, deviations on the order of 10 or 20% from the harmonic trap will be necessary at distances on the order of the oscillator length [11]. Since such anharmonic deviation should be clearly visible in the experimental analysis, we have to conclude that a clear explanation for the main part of the observed discrepancy between theoretical and experimental results is still to be found.

4. DYNAMICAL BEHAVIOR OF ATOMIC BOSE-EINSTEIN CONDENSATES

Our aim in this section is to present a study about the dynamical stability of a condensate in the presence of

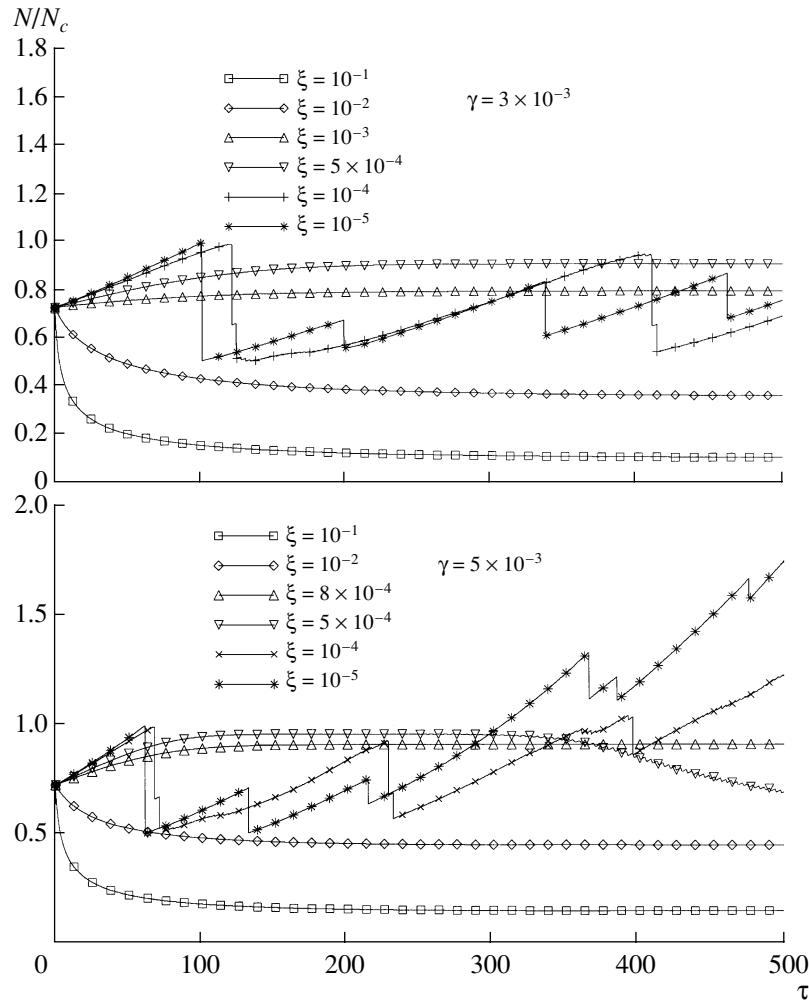


Fig. 4. Time evolution of the number of particles in the condensate state normalized by the initial number one (N/N_0) as a function of the dimensionless time $\tau \equiv \omega t$. In the upper panel, representing the case $\gamma = 3 \times 10^{-3}$ and a set of values of ξ , we can verify decay, sequences of growths and collapses, and formation of autosolitons. In the lower panel, with $\gamma = 5 \times 10^{-3}$, we note decreasing N , autosolitons, and sequences of collapses with chaotic behavior (as for $\xi = 10^{-5}$).

atomic feeding and dissipation processes. We have considered the extended version of the Gross–Pitaevskii equation, given by Eq. (1), with nonzero dissipative terms, and have considered the spherically symmetric case. In particular, we assumed consideration of a more realistic case, with $\lambda_3 = 0$. For the atomic dissipation, we assumed that only the term G_ξ is nonzero, corresponding to three-body recombination, since the contribution of the other dissipative term, due to dipolar relaxation, is usually considered to be much smaller.

The time evolution of the observables that we have studied, such as the mean square radius and the number of atoms, was extended up to $\omega t = 500$. A wide range of values for the nonconservative parameters was explored after we have realized the rich dynamical structure presented by (1). For convenience, the non-conservative parameters related to feeding and dissipation were, respectively, replaced by dimensionless

parameters, given by $\gamma \equiv 2G_\gamma/(\hbar\omega)$ and $\xi \equiv G_\xi(m\omega/\hbar)^2/[(4\pi|a|)^2(2\hbar\omega)]$. We have observed that, in the long-time evolution, depending on the relation between γ and ξ , the solutions can be very unstable and chaotic, as well as very stable, solitonic-like solutions. We have explored numerically the dynamical solutions of (1), for γ and ξ covering a wide region from 10^{-1} to 10^{-5} , considering the actual perspective of experiments with BEC, in which it is possible to vary the two-body scattering length from positive to negative values. We have mainly been interested in verifying the parametric regions, defined by γ and ξ , where the equation gives stable or unstable solutions. The results are presented in a diagrammatic form in Fig. 3. The upper-left part is the region where the solutions are stable (small feeding, with increasing dissipation), and the lower-right part is the more unstable region (large values for the feeding parameter, with less dissipation).

Typical behaviors of the time evolution of the number of particles for fixed values of the feeding parameter, $\gamma = 0.003$ and $\gamma = 0.005$, and for several values of the dissipation parameter ξ are shown in two panels of Fig. 4. In the upper panel, we notice that the system can show collapsing behavior when the relation between the feeding parameter and dissipation is large. In the case where the feeding is further increased, as shown in the lower frame, we have also observed cases where the maximum critical number N_c is no longer restricted, with a clear indication that higher radial modes are populated. In order to make a stability analysis of the equation and verify the possible occurrence of chaotic behaviors, we have considered the Deissler–Kaneko criterion [15], which corresponds to a calculation of extended Lyapunov exponents. Chaotic behaviors are identified by a positive slope of the exponents in the time evolution. As a general remark, we have observed that, in the regime of small feeding ($\gamma \leq 10^{-4}$), the extended Lyapunov exponent shows no positive slope (no chaos). However, for larger values of γ/ξ , from $\gamma \sim 10^{-3}$ to 10^{-1} , we have verified a complex dynamics, with the occurrence of collapses and chaos [8, 9].

5. CONCLUSION

In summary, we reported here a few results of our investigation on the stability of atomic condensed systems, with negative two-body scattering length, considering extensions of the GP formalism. The maximum critical number of particles was studied by considering the stationary version of the formalism. We studied the effect in the critical number due to deviations from the spherical symmetry in the harmonic trap, as well as the effect of trap deformation caused by anharmonic terms. In the static case, we also considered the effect of an elastic three-body interaction in the system. We observed that, for a range of values of this interaction, there exists a transition similar to the liquid–gas phase transition.

In the dynamical cases, we solved the nonconservative Gross–Pitaevskii equation with inelastic three-body interactions and atomic amplification from the external cloud. In this case, we observed interesting dynamics, leading to chaotic behavior or very stable, solitonic-like, solutions. The chaotic behavior was observed mainly when the feeding parameter (linear term, in the NLSE) was about two orders of magnitude larger than the dissipation parameter (quintic term in the NLSE). Also observed were weak and strong instabilities (causing collapses and growth–collapse cycles).

In some cases, “autosoliton” solutions were observed, with final stabilization of the system, with equilibrium between feeding and dissipation processes.

ACKNOWLEDGMENTS

We express our thanks to Fundação de Amparo à Pesquisa do Estado de São Paulo (FAPESP) and Conselho Nacional de Desenvolvimento Científico e Tecnológico (CNPq) of Brazil for partial support.

REFERENCES

1. Anderson, M.H., Ensher, J.R., Matthews, M.R., *et al.*, 1995, *Science*, **269**, 198.
2. Mewes, M.-O., Andrews, M.R., van Druten, N.J., *et al.*, 1996, *Phys. Rev. Lett.*, **77**, 416.
3. Bradley, C.C., Sackett, C.A., and Hulet, R.G., 1997, *Phys. Rev. Lett.*, **78**, 985; Sackett, C.A., Bradley, C.C., Welling, M., and Hulet, R.G., 1997, *Braz. J. Phys.*, **27**, 154.
4. Ruprecht, P.A., Holland, M.J., Burnett, K., and Edwards, M., 1995, *Phys. Rev. A*, **51**, 4704.
5. Courteille, P.W., Bagnato, V.S., and Yukalov, V.I., 2001, *Laser Phys.*, **11**, 659; Dalfovo, F., Giorgini, S., Pitaevskii, L.P., and Stringari, S., 1999, *Rev. Mod. Phys.*, **71**, 463.
6. Roberts, J.L., Claussen, N.R., Cornish, S.L., *et al.*, 2001, *Phys. Rev. Lett.*, **86**, 4211.
7. Gammal, A., Frederico, T., and Tomio, L., 1999, *Phys. Rev. E*, **60**, 2421; Gammal, A., Frederico, T., Tomio, L., and Chomaz, P., 1999, *Phys. Rev. A*, **61**, 051602R; Gammal, A., Frederico, T., Tomio, L., and Chomaz, P., 2000, *J. Phys. B: At. Mol. Opt. Phys.*, **33**, 4053.
8. Filho, V.S., Gammal, A., Tomio, L., and Frederico, T., 2000, *Phys. Rev. A*, **62**, 033605.
9. Filho, V.S., Frederico, T., Gammal, A., and Tomio, L., 2002, *Phys. Rev. E* (in press); *Preprint*, cond-mat/0207403.
10. Gammal, A., Frederico, T., and Tomio, L., 2001, *Phys. Rev. A*, **64**, 055602;
11. Filho, V.S., Gammal, A., and Tomio, L., 2002, *Phys. Rev. A* (in press); *Preprint*, cond-mat/0208231.
12. Gammal, A., Tomio, L., and Frederico, T., 2002, *Phys. Rev. A* (in press).
13. Filho, V.S., Abdullaev, F.K., Gammal, A., and Tomio, L., 2001, *Phys. Rev. A*, **63**, 053603.
14. Gammal, A., Frederico, T., Tomio, L., and Abdullaev, F.K., 2000, *Phys. Lett. A*, **267**, 305; Abdullaev, F.K., Gammal, A., Tomio, L., and Frederico, T., 2001, *Phys. Rev. A*, **63**, 043604.
15. Deissler, R.J. and Kaneko, K., 1987, *Phys. Lett. A*, **119**, 397.